Prediction of Chaotic Dynamics in Sheared Liquid Crystalline Polymers

M. Grosso* and R. Keunings
CESAME Unité de Mécanique Appliquée, Université Catholique de Louvain, Avenue G. Lemaitre 4-6, B-1348, Louvain La-Neuve, Belgium

S. Crescitelli
Dipartimento di Ingegneria Chimica, Università Federico II di Napoli, Piazzale Tecchio 80, I-80125, Napoli, Italia

P. L. Maffettone†
Dipartimento di Scienza dei Materiali ed Ingegneria Chimica, Politecnico di Torino, Corso Duca degli Abruzzi 24, I-10129 Torino, Italia
(Received 3 November 2000)

A rheological model for rodlike polymers in the nematic liquid-crystalline phase is analyzed to characterize irregular dynamical response under pure shear flows. The model is studied with a continuation approach, and a period doubling scenario is detected. Time series generated via simulation are studied with nonlinear analysis tools to prove the existence of chaotic regimes.

DOI: 10.1103/PhysRevLett.86.3184 PACS numbers: 83.80.Tc

Polymers in the nematic phase show several peculiar rheological features that are due to both intrinsic anisotropy of the molecules and the presence of spatial variation of molecule average orientation in the bulk. These phases are successfully described with a molecular model [1,2]. The rodlike molecules are treated as rigid rods, and the sample is described with an orientational distribution function. The sample evolution is predicted with a continuity equation for the distribution function (a Fokker-Planck equation) that accounts for thermal agitation, excluded volume effects, and macroscopic flow. The stress tensor is calculated once the distribution function is known as derived by Doi and Edwards [3]. The coupling of the continuity equation for the distribution function and the stress equation gives a rheological constitutive equation for rodlike polymers. In its homogeneous formulation, the model is capable of describing the stress response at intermediate and high shear rates—that is, when spatial distortion effects can be neglected [4,5].

Some recent time resolved measurements [6] of the linear conservative dichroism on liquid crystalline polymers (a lyotropic solution of polybenzylglutamate in *m* cresol) subjected to shear flows show an irregular response at intermediate shear rates, which could be attributed to chaotic behavior. Strange dynamics have also been experimentally reported by Bandyopadhyay *et al.* [7], who detected a chaotic dynamics at high shear rates in a system consisting of wormlike micelles that could be in the nematic phase. It is worth remarking that Bandyopadhyay *et al.* attributed the inception of chaotic dynamics to shear banding.

Those observations motivated the present investigation on the rigid rod model in order to prove whether chaotic behavior is indeed predicted. The sample is described with a population of rigid rods [1,2]. The orientational distribution function $\psi(\mathbf{u}, t)$ gives the probability density that a rod, at time t, is oriented along the direction specified by the pseudoversor $\mathbf{u}$. In dimensionless form, the continuity equation for the orientational distribution function is

$$\frac{\partial \psi}{\partial t} = \frac{\partial}{\partial \mathbf{u}} \cdot \left[\frac{\partial \psi}{\partial \mathbf{u}} + \frac{\psi}{k_B T} \frac{\partial V(\mathbf{u})}{\partial \mathbf{u}} - (\mathbf{K} \cdot \mathbf{u} - \mathbf{uuu} : \mathbf{K})\psi \right]. \quad (1)$$

In Eq. (1), t is time made dimensionless with an average rotational diffusivity (not appearing in the equation), $k_B T$ is the Boltzmann factor, $V(\mathbf{u})$ represents a mean-field nematic potential, and $\mathbf{K}$ is the dimensionless velocity gradient. The partial derivative with respect to $\mathbf{u}$ represents the gradient over the unit sphere. It should be remarked that Eq. (1) is written by assuming constant rotational diffusivity, and rods with infinite aspect ratio. The nematic potential here considered is the Maier-Saupe [8] one:

$$V(\mathbf{u}) = -\frac{3}{2} U k_B T \langle \mathbf{uu} \rangle : \mathbf{uu}, \quad (2)$$

where U is the intensity of the nematic field, and the brackets imply ensemble average. The other important parameter is the nondimensional (through the rotational diffusivity) shear rate G contained in the velocity gradient. The velocity of the shear flow here considered is given by $\mathbf{v} = [Gz, 0, 0]$; thus, x is the flow direction, y is the vorticity direction, and z is the velocity gradient direction. In the following, the plane xz will be referred to as the shearing plane.

Equation (1) is reduced to a set of ordinary differential equations (ODEs) through a Galerkin scheme [5] once the distribution function is expanded in the eigenfunctions of the Laplacian operator in spherical coordinates, i.e., in

 0031-9007/01/86(14)/3184(4)$15.00

spherical harmonics:

$$\psi(t;\mathbf{u}) = \sum_{\substack{l=0 \\ \text{even}}}^{\infty} \sum_{m=-l}^{l} b_{l,m}(t) Y_{lm}(\mathbf{u}) . \quad (3)$$

In Eq. (3), the coefficients $b_{l,0}$ are real, and the rest of them are in general complex; they are all real if the distribution function is symmetric with respect to the xz plane. Only even l indices are needed for the antipodal symmetry of the distribution function. Furthermore, since the distribution function is real, the following relation holds:

$$b_{l,-m} = (-1)^m b^*_{l,m} . \quad (4)$$

By truncating the expansion to some level n, one ends up with a finite set of ODEs. The truncation level is chosen to ensure discretization convergence, and it proved sufficient to deal with $n = 10$ for the parameter values here investigated; in fact, the results were quantitatively confirmed also with $n = 12$. A system consisting of 5 real and 30 complex ODEs is obtained with $n = 10$. Two parameters, U and G, appear in the model. The resulting dynamical system is 65 dimensional, the $b_{l,m}$ coefficients being the state variables.

Solution diagrams were obtained with a continuation algorithm [9] (AUTO97 [10]). With the continuation technique, one starts from a known stationary or periodic solution, and follows the solution curve as one parameter value is gradually changed. During the continuation process, bifurcation points are detected as they are encountered. With this approach, however, only stationary and periodic solutions can be found, while quasiperiodic and chaotic solutions cannot be traced out.

Figure 1 shows the solution diagram for $U = 5.27$. For the sake of illustration, the imaginary part of $b_{2,2}$ is reported versus the nondimensional shear rate. For this U value the system is predicted to be in the nematic phase at rest ($G = 0$). The solution structure is very similar to that of Fig. 4 of Faraoni *et al.* [11] that was calculated at a slightly different U value ($U = 5.33$). The reader should refer to that paper for a detailed description of the solution diagram structure; suffice to mention that whenever the imaginary part of $b_{2,2}$ is nonzero the distribution function is not symmetric with respect to the shearing plane, and the average orientation is out of that plane. Flow-aligning (stationary) solutions are found at high shear rates, whereas time periodic solutions are predicted at low shear rates. However, an important difference is the appearance of harmonic cascades departing from the out-of-plane oscillating branches at intermediate shear rates, while in Faraoni *et al.* only 2 period oscillations are found at that different U-value. The harmonic cascades are qualitatively reported in the insets of Fig. 1. It is worth noting that the two cascades are qualitatively identical since they represent two mirror symmetric solutions with respect to the shearing plane.

Figure 2 shows the evolution of the average sample orientation plotted onto the unit sphere for the periodic solutions within the harmonic cascade. The results have been obtained by integrating the ODEs with an adaptive time step Runge-Kutta-Verner fifth and sixth order method. The average orientation here chosen is the eigenvector corresponding to the largest eigenvalue of the second rank orientation tensor $\langle \mathbf{uu} \rangle$. This quantity at equilibrium ($G = 0$) gives the director orientation. It is apparent that the average orientation lays out of the shearing plane, eventually experiencing very complex oscillations (Fig. 2d). The G values corresponding to the period doubling bifurcations and an estimation of the Feigenbaum number [12] are reported

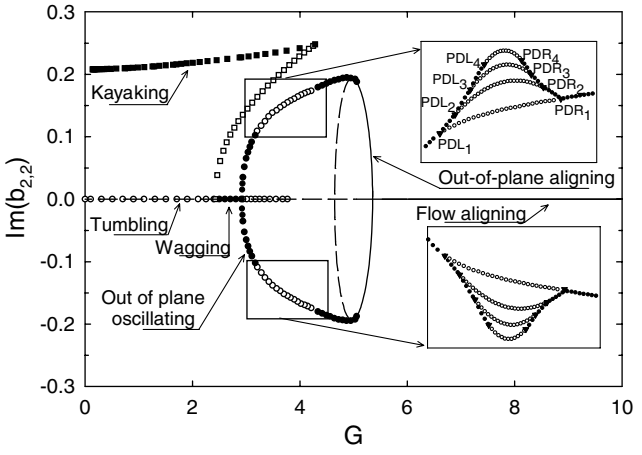

FIG. 1. The solution diagram for $U = 5.27$ (solid line: stable stationary solutions; dashed lines: unstable stationary solutions; ●: stable periodic solutions; ○: unstable periodic solutions; ■: stable period 2 solutions; □: unstable period 2 solutions). For periodic solutions the maximum attained during the oscillation is reported. The inset reports qualitatively the period doubling cascades. Types of solutions are reported.

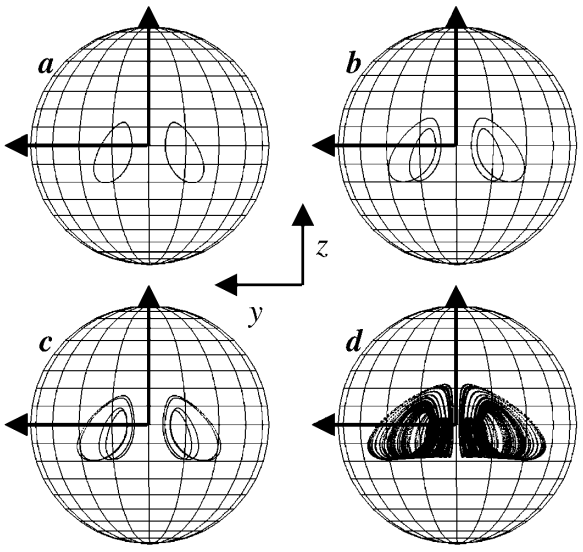

FIG. 2. The trajectories of the eigenvector corresponding to the largest eigenvalue of $\langle \mathbf{uu} \rangle$ after the transient. The orbits are plotted over the unit sphere. (a) $G = 3.15$; (b) $G = 3.20$; (c) $G = 3.23$; (d) $G = 3.30$.

TABLE I. The G values corresponding to period doubling bifurcations in the harmonic cascade. The third column reports the estimation of the Feigenbaum number.

Label	G	$\frac{G_i-G_{i-1}}{G_{i+1}-G_i}$
PDL_1	3.162 102	...
PDL_2	3.228 629	4.1875
PDL_3	3.244 516	4.5903
PDL_4	3.247 977	4.6519
PDL_5	3.248 721	...
PDR_1	4.271 441	...
PDR_2	4.193 733	5.3217
PDR_3	4.179 131	4.6967
PDR_4	4.176 022	...

in Table I. It so appears that these successive estimates are approaching the limiting value (4.6692...) typical of most period doubling chaotic scenarios. Again, it should be remarked that the spherical harmonic truncation has no impact on the period doubling cascade, in fact, bifurcation points calculated with $n = 12$ differ at most by 0.025%.

To elucidate on possible chaotic dynamics, time series of state variables generated via simulation were studied. This approach was implemented because system high dimensionality makes its direct analysis cumbersome. The $b_{2,0}$ coefficient was monitored with a nondimensional time sampling rate $\Delta t = 0.025$. Indeed, only one state variable was tracked since the attractor can be reconstructed from it on the basis of embedding theorems [13,14]. These theorems state, under generic conditions, that the attractor in the original phase space has a one-to-one image in the so-called embedding space. The trajectory in this new space consists of vectors given by

$$\mathbf{s}_n = [s_{n-(m-1)\tau}, s_{n-(m-2)\tau}, \ldots, s_n], \qquad (5)$$

where m represents the embedding dimension, and τ is the so-called time delay. The time series analysis has been accomplished with the package TISEAN [15] to obtain a Poincaré section, an estimation of the largest Lyapunov exponent, and the attractor correlation dimension. The time delay was measured with the mutual information technique [16], and confirmed with the correlation function theory [17] ($\tau \sim 55$ for the chosen Δt). Once the delay time was known, the embedding dimension was determined with the false nearest neighbor approach [18]. For $G = 3.44$, that is well within the harmonic cascade, the embedding dimension was found to be $m = 4$. With the time delay and the embedding dimension it is possible to reconstruct a Poincaré section of the attractor. This map was obtained by choosing as position of the crossing the average of the data, and its projection onto the plane $s_t s_{t+\tau}$ is reported in Fig. 3. It is apparent that a very complex structure is found.

The estimation of the largest Lyapunov exponent was performed with the method proposed by Kantz [19]. Figure 4 reports the logarithm of the stretching factor versus

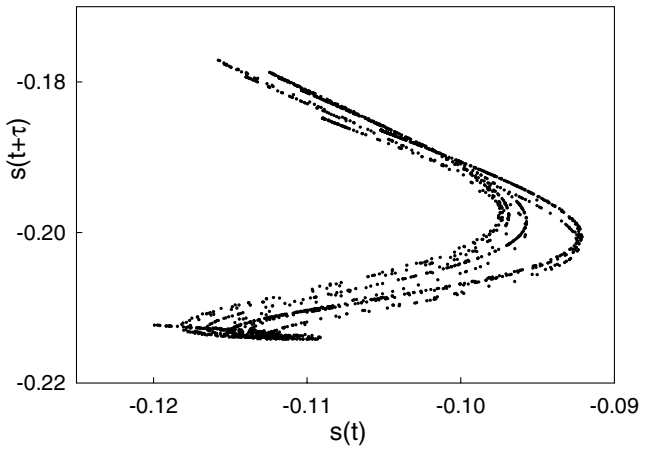

FIG. 3. A Poincaré section for $G = 3.44$.

an iteration number for different embedding dimensions. It is worth remarking that the slope at intermediate iterations saturates for an embedding dimension of 4 thus confirming the false nearest neighbor result. This slope for $m \geq 4$ gives an estimation of the dominant Lyapunov exponent. This quantity is positive ($\sim$0.232), and thus predicts a chaotic dynamics [20].

Finally, the attractor correlation integral [21] is illustrated in Fig. 5. The correlation dimension is the slope of the curves in the linear range. Data for different embedding dimensions are reported. Again, the slope is found to saturate for $m \geq 4$, and it is ca. 2.24, confirming the fractal nature of the attractor.

To conclude, we have proved the existence of a chaotic regime in a constitutive equation for nematic liquid crystalline polymeric mesophases subjected to constant shear flows. The model is specified by assuming spatial uniformity, rods with infinite aspect ratio, and constant average

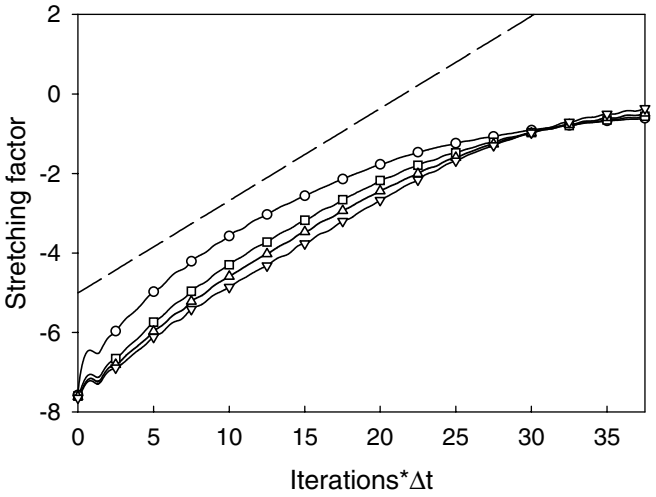

FIG. 4. The stretching factor versus iteration for $G = 3.44$. Results for different embedding dimensions are illustrated (○: $m = 3$; □: $m = 4$; ▽: $m = 5$; △: $m = 6$). The dashed line indicates the slope at intermediate iterations for $m \geq 4$.

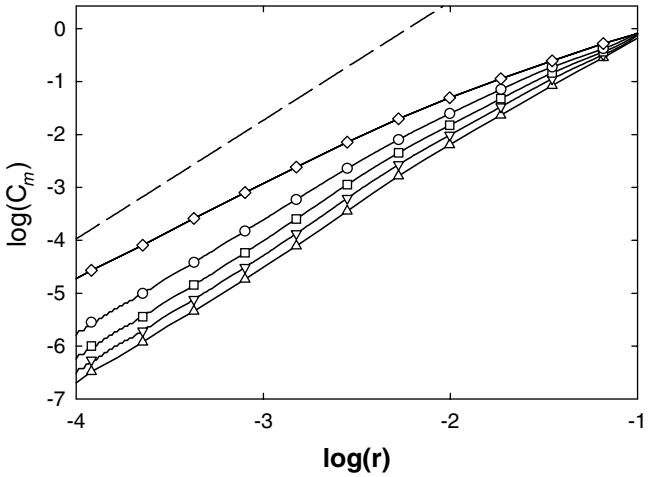

FIG. 5. The correlation integral for $G = 3.44$. Results for different embedding dimensions are illustrated ($\diamond$: $m = 2$; $\bigcirc$: $m = 3$; $\square$: $m = 4$; $\triangledown$: $m = 5$; $\triangle$: $m = 6$). The dashed line indicates the slope in the linear range for $m \geq 4$.

rotational diffusivity. The chaotic window emerges from a period doubling cascade at intermediate shear rates — that is, in a shear rate range where the rheological predicting capabilities of the model are significant. The chaotic regime is due to the nonlinearities present in the excluded volume mean field [Eq. (2)]. Note, finally, that experimental results [6,22] show irregular responses at shear rates slightly below the flow aligning regime in good agreement with the present theoretical predictions.

Work supported in part by the ARC 97/02-210 project, Communaute Francaise de Belgique, and by TMR Rheology of liquid crystals C. N. FMRX-CT96-0003.

*Present address: Dipartimento di Ingegneria Chimica, Università Federico II di Napoli, Piazzale Tecchio 80, I-80125, Napoli, Italia.

†Corresponding author.

[1] S. Z. Hess, Naturforsch. A **31**, 1034 (1976).
[2] M. Doi, J. Polym. Sci. Polym. Phys **19**, 229 (1981).
[3] M. Doi and S. F. Edwards, *The Theory of Polymer Dynamics* (Clarendon, Oxford, 1986).
[4] G. Marrucci and P. L. Maffettone, Macromolecules **22**, 4076 (1989).
[5] R. G. Larson, Macromolecules **23**, 3983 (1990).
[6] J. Mewis *et al.,* Macromolecules **30**, 1323 (1997).
[7] R. Bandyopadhyay, G. Basappa, and A. K. Sood, Phys. Rev. Lett. **84**, 2022 (2000).
[8] W. Maier and A. Saupe, Naturforsch. A **14**, 882 (1959).
[9] R. Seydel, Int. J. Bifurcation Chaos Appl. Sci. Eng. **1**, 3 (1991).
[10] E. J. Doedel *et al.,AUTO97: Continuation and Bifurcation Software for Ordinary Differential Equations* (Concordia State University, Montreal, 1997).
[11] V. Faraoni *et al.,* J. Rheol. **43**, 829 (1999).
[12] M. J. Feigenbaum, J. Stat. Phys. **19**, 25 (1978).
[13] F. Takens, *Detecting Strange Attractors in Turbulence,* Lecture Notes in Mathematics (Springer, New York, 1981), Vol. 898.
[14] T. Sauer, J. Yorke, and M. Casdagli, J. Stat. Phys. **65**, 579 (1991).
[15] R. Hegger, H. Kantz, and T. Schreiber, Chaos **9**, 413 (1999).
[16] A. M. Fraser and H. L. Swinney, Phys. Rev. A **33**, 1134 (1986).
[17] W. Liebert and H. G. Schuster, Phys. Lett. A **142**, 107 (1989).
[18] M. B. Kennel, R. Brown, and H. D. I. Abarbanel, Phys. Rev. A **45**, 3403 (1992).
[19] H. Kantz, Phys. Lett. A **185**, 77 (1994).
[20] S. Wiggins, *Introduction to Applied Nonlinear Dynamical Systems and Chaos* (Springer, New York, 1990).
[21] P. Grassberger and I. Procaccia, Physica (Amsterdam) **9D**, 189 (1983).
[22] J. Vermant (personal communication).